CYBERNETICS AND PHYSICS, VOL. 11, NO. 4, 2022, 246–252

VIBRATION FIELD CONTROL OF A TWO-ROTOR VIBRATORY UNIT IN THE DOUBLE SYNCHRONIZATION MODE

Olga P. Tomchina
Saint Petersburg State University of Architecture and Civil Engineering (SPSUACE),
2-nd Krasnoarmeiskaya St. 4, 190005, St. Petersburg, Russian Federation
otomchina@mail.ru

Article history:
Received 12.12.2022, Accepted 25.12.2022

Abstract

In the paper the problem of feedback control of vibrational fields in a vibration unit in the double synchronization mode is studied. The algorithms for control of the vibration fields by means of the control of the phase shift between rotors are proposed. The performance of the closed loop mechatronic systems is examined by simulation for the model of the two-rotor vibration unit SV-2M.

1 Introduction

Many interesting physical phenomena can be found in such complex nonlinear systems as vibration units (VU). VU are used in the mining and manufacturing industries for the purpose of transporting and processing of materials or products: grinding, screening, mixing, compacting, etc. [Chelomey, 1981]. Very often the vibrational transportation is also used. And separation of bulk materials by fractions are vibrating screens that have a moving screening surface (platform) as their working body [Blekhman et al., 2001; Firsova, 2002b; Firsova, 2002a]. The VU is usually equipped with electromechanical vibration actuators made on the basis of unbalanced rotors driven by electric drives.

Since different points of a vibrating body oscillate along different trajectories, one may speak about vibrational fields of VU [Chelomey, 1981]. A systematic approach to analysis and synthesis of the vibrational fields for vibrating units was proposed by I.I.Blekhman with coauthors in 2001-2003 [Blekhman et al., 2001; Firsova, 2002b; Firsova, 2002a] based on the approach of the vibrational mechanics [Blekhman, 2000]. It was experimentally confirmed that the inhomogeneity of the vibration field and the more complex trajectories of motion of various points of the platform, primarily in the screens, make it possible to obtain useful technological effects [Blekhman and Vaisberg, 2011].

In [Chelomey, 1981], the problem of constructing a plane-parallel field of trajectories of the points of the platform of a one-rotor vibrational machine is solved by means of an eccentric arrangement of the vibrator. In the simplest case, when the vibrator is positioned at the center of mass, the platform performs plane-parallel circular translational oscillations and the trajectory of any of its points in the vertical plane is described by the equation of circles having the same parameters, that is, the created field of vibrations is homogeneous. With the eccentric location of the actuator, the points of the platform oscillate along trajectories close to elliptical ones, and the ratios and absolute sizes of the axes of the ellipses differ for different points, that is, the vibration fields are inhomogeneous.

In [Blekhman et al., 2001; Firsova, 2002b; Firsova, 2002a] the construction of a vibration field for a VU with two actuators is studied. It is shown that it is possible to obtain a more diverse picture of the fields of trajectories in comparison with one-rotor installations. The problem of synthesis and analysis of vibration fields is considered and universal field diagrams are constructed. It is shown that the vibration field of the two-rotor vibration system depends on the coordinates of the points of fastening of the rotors, the mass of the debalances and the steady phase difference of the debalances provided they are in stable synchronous rotation mode.

In [Rumyantsev and Tarasov, 2010] is shown that using three actuators may further increase efficiency of the vibration transportation. The diagram of the motion of various points of the supporting body for three-rotor machine is shown in Fig. 1. Movement in the area of bulk material loading in this motion pattern is predominantly in the horizontal direction, which allows more efficient unloading of the hopper. Then the transported material, advancing along the working surface, begins to experi-

ence more and more the influence of the vertical component, and on arrival at the unloading right part, the material is thrown up to maximum, which ensures the most effective screening.

Additional possibilities for stabilization of synchronous modes of rotation actuators provide improvement of the control algorithms. One of the most effective methods for creating inhomogeneous oscillation fields is the use of special synchronization algorithms that stabilize the rotation of unbalanced rotors with a given steady phase difference, since this mode obviously introduces asymmetry into the movement of the platform. Synchronization of the three-rotor unit and the stability of the synchronous state is studied in [Zhang et al., 2012]. At present, computer technologies are widely used in engineering and one of the promising approaches is the creation of mechatronic units based on the principles of vibration control by feedback. The signals from the sensors are fed to the controlling computer, which allows to implement complex control algorithms. It would allow us to talk about the transition to a new generation of vibration equipment [Blekhman and Fradkov, 2001]. In [Tomchina, 2018] the vibration field control of a two-rotor vibratory unit in the simple synchronization mode is studied. In this paper the results of [Tomchina, 2018] are extended to the problem of vibration field control of a two-rotor vibratory unit in the double synchronization mode. The parameters of the unit model correspond to experimental vibration set-up SV-2M designed in the IPME [Blekhman et al., 1999; Andrievskii et al., 2016].

2 Two-rotor vibration unit: kinematics and dynamics

Efficiency of the proposed algorithms is analyzed for 2-rotor vibration unit model with 6 degrees of freedom taking into account 3 degrees of freedom for supporting body (Fig. 1).

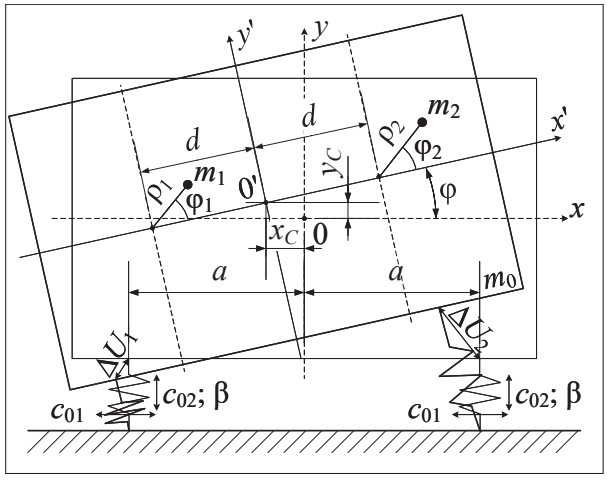

Figure 1. The kinematic scheme of controlled vibrational stand.

Here φ_1, φ_2 are the rotation angles of the rotors measured from the horizontal position, x_c, y_c are the horizontal and vertical displacement of the supporting body from the equilibrium position, $m_i = m$, are the masses of the rotors, $\varrho_i = \varrho$ is the eccentricity of rotors, c_{01}, c_{02} are the horizontal and vertical spring stiffness, m_0 is the total mass of the unit, β is the damping coefficient. We will assume that rotor shafts are orthogonal to the motion of the support.

The unit dynamics can be described by the Lagrange 2nd kind equations, see [Blekhman et al., 1999; Andrievskii et al., 2016]. It is described below for completeness.

$$
\begin{aligned}
&m_0\ddot{x}_c - \ddot{\varphi} m\varrho\left[\sin(\varphi+\varphi_1)+\sin(\varphi+\varphi_2)\right] -\\
&\ddot{\varphi}_1 m\varrho\sin(\varphi+\varphi_1) - \ddot{\varphi}_2 m\varrho\sin(\varphi+\varphi_2) -\\
&\dot{\varphi}^2 m\varrho\left[\cos(\varphi+\varphi_1)+\cos(\varphi+\varphi_2)\right] -\\
&\dot{\varphi}_1^2 m\varrho\cos(\varphi+\varphi_1) - \dot{\varphi}_2^2 m\varrho\cos(\varphi+\varphi_2) -\\
&2\dot{\varphi}\dot{\varphi}_1 m\varrho\cos(\varphi+\varphi_1) -\\
&2\dot{\varphi}\dot{\varphi}_2 m\varrho\cos(\varphi+\varphi_2) + 2c_{01}x_c + \beta\dot{x}_c = 0;\\
&m_0\ddot{y}_c + \ddot{\varphi} m\varrho\left[\cos(\varphi+\varphi_1)+\cos(\varphi+\varphi_2)\right] -\\
&\ddot{\varphi}_1 m\varrho\cos(\varphi+\varphi_1) - \ddot{\varphi}_2 m\varrho\cos(\varphi+\varphi_2) -\\
&\dot{\varphi}^2 m\varrho\left[\sin(\varphi+\varphi_1)+\sin(\varphi+\varphi_2)\right] -\\
&\dot{\varphi}_1^2 m\varrho\sin(\varphi+\varphi_1) - \dot{\varphi}_2^2 m\varrho\sin(\varphi+\varphi_2) -\\
&2\dot{\varphi}\dot{\varphi}_1 m\varrho\sin(\varphi+\varphi_1) - 2\dot{\varphi}\dot{\varphi}_2 m\varrho\sin(\varphi+\varphi_2) +\\
&2c_{02}y_c + \beta\dot{y}_c = 0;\\
&-\ddot{x}_c m\varrho\left[\sin(\varphi+\varphi_1)+\sin(\varphi+\varphi_2)\right] +\\
&\ddot{y}_c m\varrho\left[\cos(\varphi+\varphi_1)+\cos(\varphi+\varphi_2)\right] +\\
&\ddot{\varphi}\left[J + J_1 + J_2 - 2dm\varrho\left(\cos\varphi_1 - \cos\varphi_2\right)\right] +\\
&\ddot{\varphi}_1\left(J_1 - dm\varrho\cos\varphi_1\right) + \ddot{\varphi}_2\left(J_2 + dm\varrho\cos\varphi_2\right) +\\
&\dot{\varphi}_1^2 dm\varrho\sin\varphi_1 - \dot{\varphi}_2^2 dm\varrho\sin\varphi_2 + 2dm\varrho\dot{\varphi}\dot{\varphi}_1\sin\varphi_1 -\\
&2dm\varrho\dot{\varphi}\dot{\varphi}_2\sin\varphi_2 + m\varrho g\left[\cos(\varphi+\varphi_1)+\right.\\
&\left.\cos(\varphi+\varphi_2)\right] + c_{03}\varphi + \beta\dot{\varphi} = 0;\\
&-\ddot{x}_c m\varrho\sin(\varphi+\varphi_1) + \ddot{y}_c m\varrho\cos(\varphi+\varphi_1) +\\
&\ddot{\varphi}\left(J_1 - dm\varrho\cos\varphi_1\right) + \ddot{\varphi}_1 J_1 - \dot{\varphi}^2 dm\varrho\sin\varphi_1 +\\
&m\varrho g\cos(\varphi+\varphi_1) + k_c\dot{\varphi}_1 = M_1;\\
&-\ddot{x}_c m\varrho\sin(\varphi+\varphi_2) + \ddot{y}_c m\varrho\cos(\varphi+\varphi_2) +\\
&\ddot{\varphi}\left(J_2 + dm\varrho\cos\varphi_1\right) + \ddot{\varphi}_2 J_2 + \dot{\varphi}^2 dm\varrho\sin\varphi_2 +\\
&m\varrho g\cos(\varphi+\varphi_2) + k_c\dot{\varphi}_2 = M_2;
\end{aligned}
\tag{1}
$$

where J_1, J_2 are the inertia moments of the rotors, g is the gravitational acceleration, k_c is the friction coefficient in the bearings, M_1, M_2 are the motor torques (controlling variables). Kinetic and potential energies T and Π are as follows:

$$
\begin{aligned}
&T = 0.5m_0\left(\dot{x}_c^2+\dot{y}_c^2\right)+0.5\dot{\varphi}^2\left(J+J_1+J_2-\right.\\
&\left.2dm\varrho\left(\cos\varphi_1-\cos\varphi_2\right)\right)+0.5J_1\dot{\varphi}_1^2+0.5J_2\dot{\varphi}_2^2+\\
&\dot{\varphi}\dot{\varphi}_1\left(J_1-dm\varrho\cos\varphi_1\right)+\dot{\varphi}\dot{\varphi}_2\left(J_2+dm\varrho\cos\varphi_2\right)-\\
&\dot{x}_c\dot{\varphi}m\varrho\left(\sin\left(\varphi+\varphi_1\right)+\sin\left(\varphi+\varphi_2\right)\right)+\\
&\dot{y}_c\dot{\varphi}m\varrho\left(\cos\left(\varphi+\varphi_1\right)+\cos\left(\varphi+\varphi_2\right)\right)-\\
&\dot{x}_c\dot{\varphi}_1m\varrho\sin\left(\varphi+\varphi_1\right)+\dot{y}_c\dot{\varphi}_1m\varrho\cos\left(\varphi+\varphi_1\right)-\\
&\dot{x}_c\dot{\varphi}_2m\varrho\sin\left(\varphi+\varphi_2\right)+\dot{y}_c\dot{\varphi}_2m\varrho\cos\left(\varphi+\varphi_2\right),\\
&\Pi = m_0gy_c+m\varrho g\left(\sin\left(\varphi+\varphi_1\right)+\sin\left(\varphi+\varphi_2\right)\right)+\\
&c_{01}\left(x_c^2+\alpha^2\cos^2\varphi\right)^2+c_{02}\left(y_c^2+\alpha^2\sin^2\varphi\right)^2,\\
&H = T+\Pi.
\end{aligned}
\tag{2}
$$

The parameter values correspond to the vibration stand SV-2M designed in the IPME [Blekhman et al., 1999; Andrievskii et al., 2016].

3 Integral-differential speed-gradient control algorithms for double synchronization of two-rotor vibration unit

In this paper double Frequency synchronization for two-rotor vibration unit is defined as an exact coincidence of reduced angular velocities of the unbalanced rotors $\omega_s = \frac{\omega_r}{2}$; $s, r = 1, 2$ [Blekhman, 2000]. or practice approximate synchronization conditions are more appropriate [Blekhman and Fradkov, 2004]:

$$
\left|\omega_s - \frac{\omega_r}{2}\right| \le \varepsilon, \tag{3}
$$

where $\varepsilon > 0$ can be chosen numerically as $\varepsilon = 0.05\omega^*$, with a given accuracy, similar to conventional transient process measurement. However the ratio (3) may be not sufficient for synchronization, since its fulfillment does not prevent the accumulation of a phase synchronization reduced error (reduced phase shift). That is why there is a need to impose additional requirements on the system phases. To this end the notion of approximate double phase synchronization is formulated as follows [Blekhman and Fradkov, 2004]:

$$
\left|\varphi_s - \frac{\varphi_r}{2} - L_{sr}\right| \le \varepsilon_1; \quad s, r = 1, 2. \tag{4}
$$

Equations (3) and (4) should hold for some $\varepsilon > 0$, $\varepsilon_1 > 0$ and some real L_{sr}.

To provide a double synchronous rotation mode of unbalanced rotors for system (1), it is suggested to use speed-gradient method with an objective functional in the following form:

$$
Q(z) = \left\{0.5(1-\alpha)\left(H-H^*\right)^2+\alpha\left(\dot{\varphi}_1 \pm \frac{\dot{\varphi}_2}{2}\right)^2\right\}, \tag{5}
$$

where $0 < \alpha < 1$ is weight coefficient; H is total mechanical energy of a system (1), H^* is the desired value of H. The speed-gradient algorithm in the finite form with the objective functional (5) is as follows [Tomchina, 2019]:

$$
\begin{aligned}
M_1 &= -\gamma_1\left\{(1-\alpha)\left(H-H^*\right)\dot{\varphi}_1+\right.\\
&\left.\frac{\alpha}{J_1}\left(\dot{\varphi}_1 \pm \frac{\dot{\varphi}_2}{2}\right)\right\};\\
M_2 &= -\gamma_2\left\{(1-\alpha)\left(H-H^*\right)\dot{\varphi}_2\pm\right.\\
&\left.\frac{\alpha}{2J_2}\left(\dot{\varphi}_1 \pm \frac{\dot{\varphi}_2}{2}\right)\right\}.
\end{aligned}
\tag{6}
$$

For our purpose the proportional-integral (PI-) control algorithm is better suited [Tomchina, 2018]

$$
\begin{aligned}
M_1 &= -\gamma_1\left\{(1-\alpha)\left(H-H^*\right)\dot{\varphi}_1+\right.\\
&\left.\frac{\alpha}{J_1}\left(\dot{\varphi}_1 \pm \frac{\dot{\varphi}_2}{2}\right)+\frac{\alpha}{J_1}\left(\varphi_1 \pm \frac{\varphi_2}{2}+\Delta\varphi_1^*\right)\right\};\\
M_2 &= -\gamma_2\left\{(1-\alpha)\left(H-H^*\right)\dot{\varphi}_2\pm\right.\\
&\left.\frac{\alpha}{2J_2}\left(\dot{\varphi}_1 \pm \frac{\dot{\varphi}_2}{2}\right)\pm\frac{\alpha}{2J_2}\left(\varphi_1 \pm \frac{\varphi_2}{2}+\Delta\varphi_2^*\right)\right\}.
\end{aligned}
\tag{7}
$$

The choice of the values $\Delta\varphi_i^*$ in the term $(\varphi_1 \pm \varphi_2/2 + \Delta\varphi_i^*)$, allows one to specify the value of the reduced phase shift $\Delta\varphi(\infty) = \varphi_1 - \varphi_2/2$.

4 Simulation results

Simulation results are obtained using the MATLAB environment. The first set of the results show the case of single synchronization with algorithm [Tomchina, 2018]

$$
\begin{aligned}
M_1 &= -\gamma_1\left\{(1-\alpha)\left(H-H^*\right)\dot{\varphi}_1+\right.\\
&\left.\frac{\alpha}{J_1}\left(\dot{\varphi}_1 \pm \dot{\varphi}_2\right)+\frac{\alpha}{J_1}\left(\varphi_1 \pm \varphi_2+\Delta\varphi_1^*\right)\right\};\\
M_2 &= -\gamma_2\left\{(1-\alpha)\left(H-H^*\right)\dot{\varphi}_2\pm\right.\\
&\left.\frac{\alpha}{J_2}\left(\dot{\varphi}_1 \pm \dot{\varphi}_2\right)\pm\frac{\alpha}{J_2}\left(\varphi_1 \pm \varphi_2+\Delta\varphi_2^*\right)\right\}.
\end{aligned}
\tag{8}
$$

for the case of identical rotors $m = 1.5$ kg, $J_i = 0.014$ kg·m^2, $m_n = 9$ kg, $\varrho = 0.04$ m, $k_c = 0.01$ J/s, $\beta = 5$ kg/s, $c_{02} = 5300$ N/m, $c_{01} = 1300$ N/m and $\Delta\varphi_1^* = -1.1$ rad are presented in Figs. 2,3.

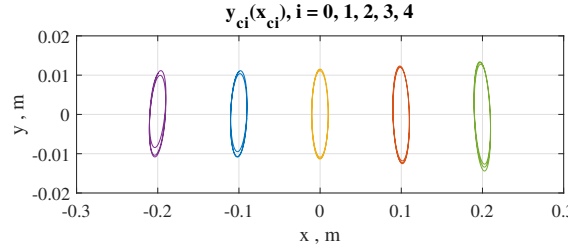

Figure 2. Diagrams of the supporting body vibration field for 5 different points of the platform ($\Delta\varphi_1^* = 1$ rad).

Fig. 2 demonstrate diagrams of the supporting body vibration field for 5 different points of the platform. The

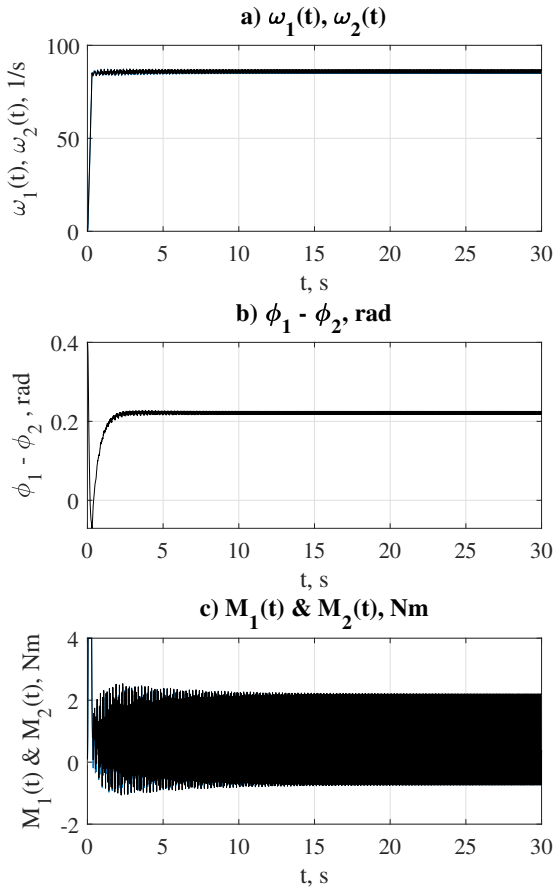

Figure 3. Simulation results for system (1), (8) with $\Delta\varphi_1^* = 1$ rad: a) $\dot{\varphi}_1(t), \dot{\varphi}_2(t)$ — rotor angular velocities; b) the phase shift $\Delta\varphi = \varphi_1 - \varphi_2$; c) M_i are controlling torques.

left trajectory corresponds to the loading end while the right trajectory corresponds to the deployment end. The diagram Fig. 2 is obtained for $\Delta\varphi_1^* = 1$ rad.

As is seen from the plots (Fig. 3) the phase synchronization takes place: $\Delta\varphi(\infty) \to L_{12} = \text{const}$. As can be seen from the graphs (Fig. 2), the vibration field when setting non-zero phase shifts $\Delta\varphi^*$, in algorithm (8) has an inhomogeneous form. The trajectory of the discharge end, which is an ellipse, has a significantly larger diameter, and the angle ψ formed by this diameter with the positive direction of the abscissa axis is obtuse (the counterclockwise direction is taken as the positive direction of the angles). This type of specified trajectory contributes to better unloading of bulk material from the platform. Note that the ordinates of the upper and lower points of this trajectory are respectively equal to: $y_{\min} = -0.0145$ m, $y_{\max} = 0.0142$ m.

In Fig. 4 a vibration field diagram for the case of double synchronization is shown, when phase shifts are specified in algorithm (7) $\Delta\varphi_1^* = 0$, $\Delta\varphi_2^* = -1.1$ rad, and in Fig. 5 and Fig. 6 a diagram of the vibration field and graphs of the change in the coordinate y_c, multiple angular velocities $\omega_1 = \dot{\varphi}_1(t)$, $\omega_2 = \dot{\varphi}_2(t)$, and reduced phase shift $\Delta\varphi = \varphi_1 - \varphi_2/2$ for given phase shifts $\Delta\varphi_1^* = 0$, $\Delta\varphi_2^* = 4$ rad are shown.

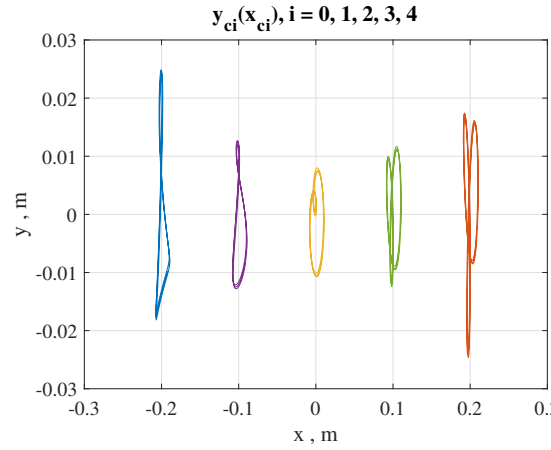

Figure 4. Simulation results for system (1), (7) with $\Delta\varphi_1^* = 0$, $\Delta\varphi_2^* = -1.1$ rad.

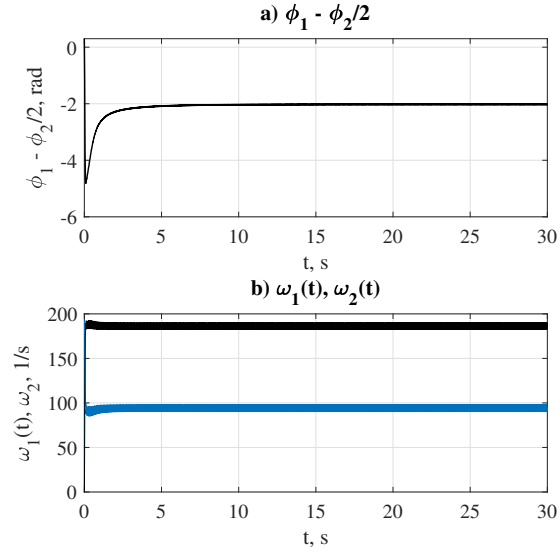

Figure 5. Simulation results for system (1), (7) with $\Delta\varphi_1^* = 0$, $\Delta\varphi_2^* = -1.1$ rad: a) $\dot{\varphi}_1(t), \dot{\varphi}_2(t)$ — rotor angular velocities; b) the reduced phase shift $\Delta\varphi = \varphi_1 - \varphi_2/2$; c) is vertical coordinate y_c.

As is seen from the graphs, the trajectories of movement of various points of the platform have a more complex form than with a single synchronization. On the right unloading end which is closer to the rotor spinning at a higher double speed ($\omega_2(t) = 2\omega_1(t)$). in

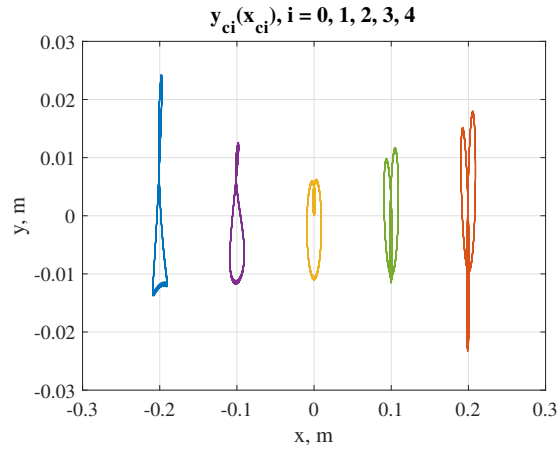

Figure 8. Simulation results for system (1), (7) with $\Delta\varphi_1^* = 0$, $\Delta\varphi_2^* = 0$.

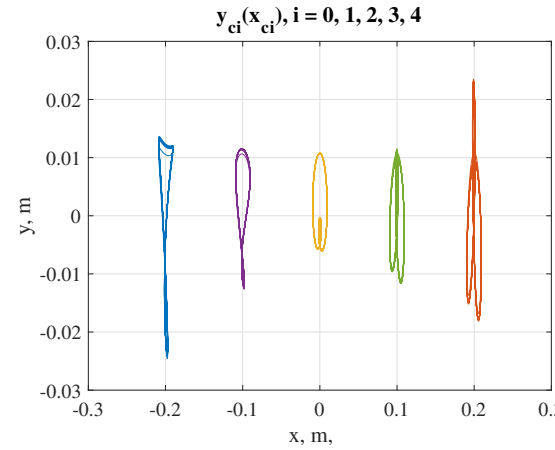

Figure 7. Simulation results for system (1), (7) with $\Delta\varphi_1^* = -4$ rad, $\Delta\varphi_2^* = 0$.

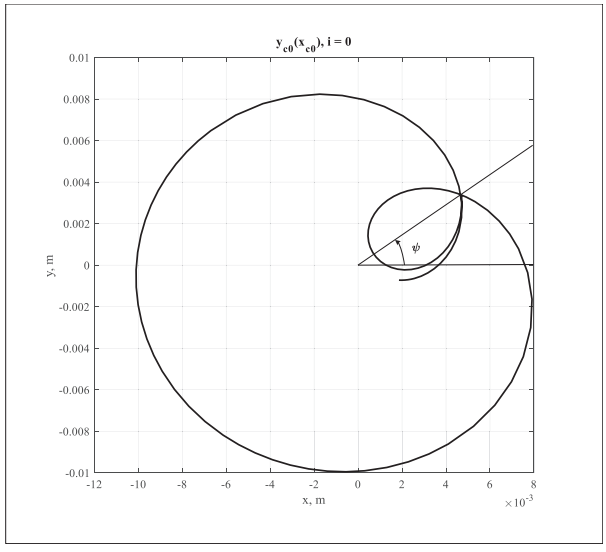

Figure 9. Definition of angle ψ.

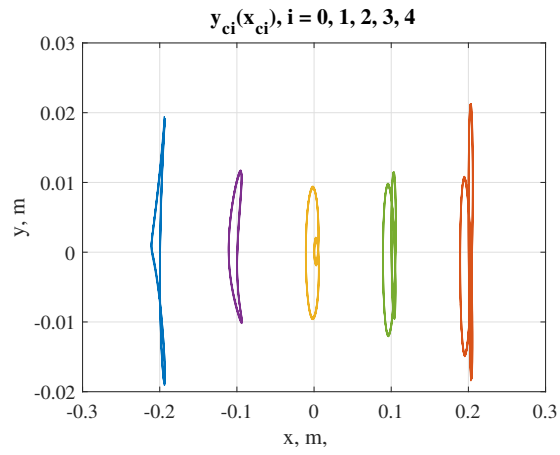

Figure 6. Simulation results for system (1), (7) with $\Delta\varphi_1^* = 6$ rad, $\Delta\varphi_2^* = 0$.

Fig. 4 the ordinate of the lower point of the trajectory is 1.5 times lower ($y_{\min} = -0.024$ m), than in the case of single synchronous mode, which improves the efficiency of unloading and prevents the formation of congestion. At the same time, the extreme left point of the platform moves along a trajectory with a sharp upward ejection, which contributes to the effective movement of the loaded bulk material along the platform. On the contrary, at $\Delta\varphi_1^* = 0$, $\Delta\varphi_2^* = 4$ rad the trajectory corresponding to the unloading end has a sharp upward projection, which prevents fast unloading. As can be seen from the graphs presented in Fig. 4— 8 and Table 1, a judgment on the type of trajectory of the unloading end can be made based on the type of trajectory of the center of mass of the platform. Let's draw a segment connecting the origin of coordinates $O(0, 0)$ and the point that is the base of the loop of the specified trajectory. Consider the angle ψ formed by this segment and the positive direction of the x-axis (Fig. 9).

Quantitatively, the dependence of the vibration field parameters on the phase shift $\Delta\varphi_i^*$ specified in the algorithm (7) is presented in Table 1. Here, the values of the given phase shifts $\Delta\varphi_i^*$, the angle of inclination of the central trajectory ψ (deg), the ordinate of the upper point of the trajectory of the loading end $y_{1\,\max}$ and the trajectory of the lower point of the unloading end $y_{2\,\min}$ are indicated. It is seen that the best type of the vibration field in terms of the efficiency of vibration transportation and the fight against congestion at the discharge end has the field shown in Fig. 4. For this case, we have: $\psi = 1300$ (2.27 rad), $y_{1\,\max} = 0.023$ m, $y_{2\,\min} = 0.024$ m. t can be concluded from Table 1, based on the simulation, that the type of vibration fields, characterized by the most effective trajectories, corresponds to a change in angle ψ in the range from 650 to 1300, which corresponds to the range $1.13 \leq \psi \leq 2.27$ rad. Figure 10 shows a graph of the dependence of the angle ψ on the phase shift $\Delta\varphi_2^*$ specified in algorithm (7) at $\Delta\varphi_1^* = 0$. With the help of such diagrams, for the desired type of vibration field, it

$\Delta\varphi_1^*$, rad	$\Delta\varphi_2^*$, rad	ψ, deg	$y_{1\,\max}$, m	$y_{2\,\min}$, m	Remark
-4.0	0	-90	0.013	0.017	1*)
3,0	0	-60	0,022	-0,017	
2,0	0	-11	0,02	-0,02	
1,0	0	45	0,019	-0,021	
0	0	90	0,021	-0,023	3*)
0	-1,1	130	0,023	-0,024	2*)
0	-1.0	120	0,022	-0,023	3*)
0	0	90	0,022	-0,023	3*)
0	1.0	82	0,022	-0,022	
0	2.0	75	0,021	-0,022	
0	3.0	65	0,021	-0,021	
0	4.0	48	0,017	-0,019	
0	5.0	23	0,016	-0,018	
0	6.0	0	0,015	-0,017	

Table 1. Notes: 1*) is the worst type of vibration field (Fig. 7); 2*) is the best view of the vibration field (Fig. 4); 3*) — is intermediate (satisfactory).

is possible to determine the required values of $\Delta\varphi_i^*$ in algorithm (7).

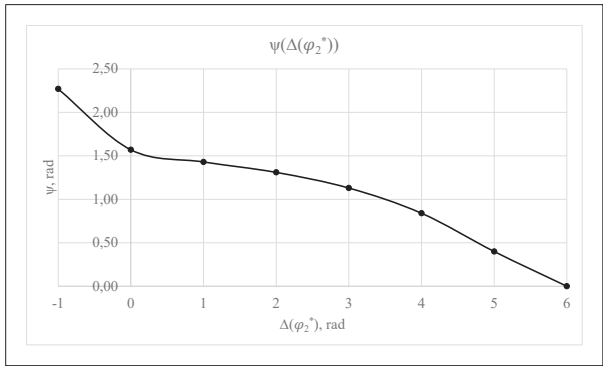

Figure 10. Graph of the dependence of angle ψ on the phase shift $\Delta\varphi_2^*$ specified in the algorithm (7) at $\Delta\varphi_1^* = 0$.

5 Conclusions

In this paper the results proposed in [Tomchina, 2018] are extended to the case of double synchronization. It is shown by simulation that the control goal is achieved with the modified algorithms of [Tomchina, 2018] . Based on the simulation, it can be concluded that the type of vibration fields characterized by the most efficient trajectories can be determined from the angle ψ calculated from the trajectory of the center of mass of the platform. This angle is formed by a segment connecting the origin of coordinates with the base of the loop of the specified trajectory and the positive direction of the abscissa axis. An interval of variation of angle ψ has been determined, which provides the best type of vibration field from the point of view of the efficiency of vibrotransportation and the fight against congestion at the unloading end. Further research may be aimed at further extension to the more complicated cases [Tomchina, 2019; Tomchina, 2020].

References

Andrievskii, B. R., Blekhman, I. I., Blekhman, L. I., Boikov, V. I., Vasil'kov, V. B., and Fradkov, A. L. (2016). Education and research mechatronic complex for studying vibration devices and processes. *J. Mach. Manuf. Reliab.*, **45** (4), pp. 369—-374.

Blekhman, I. I. (2000). *Vibrational Mechanics: Nonlinear Dynamic Effects, General Approach, Applications*. World Scientific.

Blekhman, I. I., Bortsov, Y. A., Burmistrov, A. A., Fradkov, A. L., Gavrilov, S. V., Kononov, O. A., Lavrov, B. P., Sokolov, P. V., Shestakov, V. M., and Tomchina, O. P. (1999). Computer-controlled vibrational setup for education and research. In *Proc. of 14th IFAC World Congress*, vol. M, pp. 193–197.

Blekhman, I. I. and Fradkov, A. L., editors (2001). *Control of mechatronic vibration units. (in Russian)*. St. Petersburg: Nauka.

Blekhman, I. I. and Fradkov, A. L. (2004). *On general definitions of synchronization*, pp. 179–188. Singapore: World Scientific.

Blekhman, I. I. and Vaisberg, L. A. (2011). Self-synchronization as a selforganization phenomenon and a basis for development of energy efficient technologies. In Segla, S., Tuma, J., and Petrikova, I., editors, *Proc. 10th Biennial International Conference on Vibration Problems (ICOVP), Prague, Czech Republic*, pp. 365—-370.

Blekhman, I. I., Vaisberg, L. A., and Firsova, A. (2001). Evaluation of the field of the trajectories for the body of the vibration machine with two unbalanced vibroactuators.(in russian). *Obogaschenie Rud*, **2**, pp. 39–42.

Chelomey, V. L., editor (1978—1981). *Vibration in Engineering. Handbook. (in Russian)*, vol. 4. Moscow: Machinostroenie.

Firsova, A. D. (2002a). Investigation of vibration field of a regid body set in motion by two synchronously working vibration exciters. In *Proc. of XXIX Summer school "Advanced Problems in Mechanics" (APM 2001)*, IPME RAS, pp. 231–235.

Firsova, A. D. (2002b). Stationary oscillations of the operating part of vibration machine with two arbitrary located unbalance vibration exciters. In *Book of*

Abstracts of the Annual Scientific Conference GAMM 2002, Augsburg, p. 44.

Rumyantsev, S. and Tarasov, D. (2010). Numerical simulation of nonlinear dynamics of vibration transport machines in case of three independently rotating vibration exciters. In *Recent Advances in Applied Mathematics: Proceedings of the American Conference on Applied Mathematics (AMERICAN-MATH'10)*, Harvard University, Cambridge, USA, pp. 191–194.

Tomchina, O. (2018). Control of vibrational field in a cyberphysical vibration unit. *Cybernetics and Physics*, **7** (3), pp. 144–151.

Tomchina, O. (2019). Control of vibrational field in a vibration unit: influence of drive dynamics. *Cybernetics and Physics*, **8** (4), pp. 298–306.

Tomchina, O. (2020). Control of oscillations in two-rotor cyberphysical vibration units with time-varying observer. *Cybernetics and Physics*, **9** (4), pp. 206–213.

Zhang, X., Wen, B., and Zhao, C. (2012). Synchronization of three homodromy coupled exciters in a non-resonant vibrating system of plane motion. *Acta Mechanica Sinica*, **28**, pp. 1424–1435.